CHAPTER VI. ANALYSIS OF HIGH MOLECULAR MASS INORGANIC COMPLEXES USING MATRIX-ASSISTED-LASER DESORPTION/IONIZATION (MALDI)

VI.1-- HIGH MOLECULAR WEIGHT INORGANIC COMPLEXES

Large polymetallic complexes are potentially useful molecules in a variety of areas. Photochemically active compounds are under investigation as efficient photoinitiators for solar-energy conversion,[78,79,80] catalysts, and as selective "light-activated anticancer drugs"[78]. On a molecular level, these large organometallic species typically contain light-absorbing units, central electron-collecting units, and bridges between the units.

Because of the importance of their chemical structure for optimum operation, the high molecular weight complexes must be thoroughly characterized by analytical techniques. Typical characterization techniques include NMR, electrochemistry, and X-ray crystallography. However, NMR spectra are commonly complex and suffer from paramagnetic effects[80,81] and crystals are often unobtainable. More reliable, rapid characterization is sought.

Mass spectrometry should be an effective tool in the structural characterization of these organometallic coordination complexes. However, the low volatility, fragility, and lability of the species have made MS problematic. Significant advances have been made with fast-atom-bombardment mass spectrometry (FAB-MS) and electrospray-ionization mass spectrometry (ESI-MS), although these techniques still have limitations. FAB-MS, for example, has been successful for monometallic and small polymetallic compounds, but fragmentation often causes a low intensity or complete absence of the intact molecular ion in many spectra[82,83,84]. ESI-MS suffers from similar problems, and the

[78] K. Brewer. *New Scientist*. **155** (1997) 36.

[79] R. Arakawa, R. Matsuo, K. Nozaki, T. Ohno. *Inorg. Chem.* **34** (1995) 2464.

[80] P. Didier, L. Jacquet, A. Kirsch-DeMesmaeker, R. Hueber, A. van Dorsselaer. *Inorg. Chem.* **31** (1992) 4803.

[81] R. Colton, J. Traeger. *Inorg. Chim. Acta.* **201** (1992) 153.

[82] M. Bruce, M. Liddel. *Inorg. Chim. Acta.* **198-200** (1992) 407.

[83] R. Arakawa, L. Jian, A. Yoshimura, K. Nozaki, T. Ohno, H. Doe, T. Matsuo. *Inorg. Chem.* **34** (1995) 3874.

electrospray interface can generate interferences and form new species during ionization[83]. In addition, isotopic distributions in the spectra are often complicated and unresolved.

Little work has been done with laser-based methods of MS for structural characterization of these high molecular mass polymetallic complexes. One report reveals that laser desorption decreased fragmentation and intensified the pseudomolecular ion (that is, the molecular ion with the counterions removed) peaks in comparison to FAB-MS[85]. Laser-Ionization Time-of-Flight Mass Spectrometry seems well-suited for the analysis of large organometallic species. The wide mass range of TOF-MS is ideal for the characterization of the high-mass polymetallics, and well-controlled laser ionization might decrease the fragmentation of FAB and ESI. Furthermore, even "softer" ionization might be possible by using matrix-assisted desorption/ionization methods. Matrix-assisted-laser desorption/ionization (MALDI) has reliably analyzed polymers, fragile proteins, and large biological molecules, but has not yet been exploited for other types of compounds. By analogy to the polar, easily fragmented proteins, MALDI should be useful for the fragile organometallic complexes as well.

VI.2-- MALDI

Matrix-Assisted-Laser Desorption/Ionization (MALDI) is a "soft" ionization technique that generates intact, gas-phase molecular ions of high-mass species. Combined with the nearly unlimited mass range of Time-of-Flight Mass Spectrometry, MALDI-TOF can be effective in the analysis of large, fragile molecules that fragment easily by direct laser-ionization or are above the upper mass limit of other mass spectrometric methods. Since its inception in 1987[86], most of the analytes have been high molecular weight biomolecules such as proteins, carbohydrates, and peptides. Most recently, applications have even included DNA mapping, and the mass range has

---

[84] K. Verkerk, C. de Kostor, B. Markies, J. Boersma, G. van Koten, W. Heerma, J. Haverkamp. *Organometallics.* **14** (1995) 2081.

[85] A. Bjarnson, R. Des Enfants, M. Barr, L. Dahl. *Organometallics.* **9** (1990) 657.

[86] M. Karas, D. Bachman, U. Bahr, F. Hillenkamp. *Int. J. Mass Spectrom. Ion Processes.* **78** (1987) 53.

extended to molecular weights over 1,500,000 amu[87] with sensitivities as low as femtomoles[88]. The usefulness of MALDI-TOF for biological analyses is summed up best by Cotter, who claims "one cannot overestimate the value of such instruments in the protein laboratory"[89]. In addition to biomolecules, polymer mass spectrometric studies have successfully incorporated MALDI for molecular mass and structural information.

The success of MALDI depends largely on the sample preparation procedure. In its simplest form, MALDI entails diluting the analyte in a suitable matrix and ablating the mixture. By combining a large excess of the matrix with the analyte (typical analyte:matrix ratios are 1:10 to 1:10,000), the matrix should absorb most of the ablation energy (typically UV wavelengths) rather than the analyte. The excess thermal energy imparted to the matrix causes a "soft" ejection of analyte and matrix ions into the gas phase, in contrast to a "hard" ionization process from a directly ablated sample. In addition to decreasing excess energy that might fragment the analyte, ionization is enhanced through proton transfer from the matrix to the analyte. Traditional matrices such as carboxylic acid derivatives (e.g. 2,5-dihydroxybenzoic acid) and cinnamic acid derivatives (e.g. ferulic acid, sinapic acid) have been successful in the analysis of biological material. Typically, the matrix solution is prepared in a polar organic solvent (e.g. acetonitrile, trifluoroacetic acid) and mixed with the analyte solution in a miscible solvent. The subsequent mixture is applied to the probe tip of the mass spectrometer and the solvent is evaporated. Recent innovations in sample preparation have included a "fast evaporation" method, where the matrix solution is prepared in a quickly evaporating solvent such as acetone and directly deposited on the probe tip as a dense film. The analyte solution, prepared in a solvent that will not redissolve the matrix, is applied on top of the dried matrix crystals. Advantages of this method have been improved mass accuracy and resolution[90]. For polymer analyses, non-traditional, non-polar matrices

[87] L. Latourte, J. Blais, J. Tabet. *Anal Chem.* **69** (1997) 2742.

[88] E. Nordhoff, A. Ingendoh, R. Cramer, A. Overberg, B. Stahl, M. Karas, F. Hillenkamp, P. Crain. *Rapid Commun. Mass Spectrom.* **6** (1992) 771.

[89] R. Cotter. *Anal. Chem.* **64** (1992) 1027A.

[90] O. Vorm, P. Roepstorff, M. Mann. *Anal. Chem.* **66** (1994) 3281.

such as 9-nitroanthracene have been used. The non-polar polymer analytes thus ionize via radical formation (electron abstraction) rather than by proton transfer[91].

Finding the proper matrix, solvent, and evaporation conditions that induce co-crystallization of the analyte with the matrix is essential for optimum MALDI mass spectrometry[87, 90,92, 93,94]. Ideally, the analyte incorporates itself into the crystal lattice of the matrix, and this "co-crystallization" produces a homogeneous sample surface of analyte-matrix crystals. However, this procedure is usually a "trial and error" technique and clearly "not a simple task"[94]. Even for a generally well-prepared sample surface, poorly formed crystals are dispersed throughout. The importance of sample preparation cannot be overstated since shot-to-shot reproducibility, signal intensity, mass accuracy, and resolution in MALDI spectra are governed largely by the quality of crystallization[92,95]. Only with optimal matrix formulations can analyses take advantage of the TOF instrument and the MALDI technique.

VI.3-- GOALS

Our goal is reliable mass spectral characterization of high mass inorganic complexes. Although we will concentrate on understanding a heteronuclear trimetallic species, $\{[(bpy)_2Ru(dpp)]_2IrCl_2\}(PF_6)_5$, where dpp is the bridging ligand 2,3-bis-2′-pyridylpyrazine and bpy is 2,2′-bipyridine, eventual applications could include LI-TOF-MS analyses of multimetallic compounds that incorporate more than three metals. Novel sample preparation methods including MALDI will be explored for improved mass spectral results. In contrast to the traditional, organic MALDI samples, the applicability of matrix-assisted sample preparation to organometallic complexes will be assessed.

---

[91] R. Juhasz, C. Costello. *Rapid Commun. Mass Spectrom.* **7** (1993) 343.
[92] R. Whittal, D. Schriemer, L. Li. *Anal. Chem.* **69** (1997) 2734.
[93] B. Rosinske, K. Strupar, F. Hillenkamp, J. Rosenbach, N. Dencher, U. Kruger, H. Golla. *J. Mass Spectrom.* **30** (1995) 1492.
[94] C. Vera, R. Zubarev, H. Ehring, P. Hadanssen, B. Sunqvist. *Rapid Commun. Mass Spectrom.* **10** (1996) 1429.
[95] A. J. Nicola, A. I. Gusev, A. Proctor, E. Jackson, D. Hercules. *Rapid Commun. Mass Spectrom.* **9** (1995) 1164.

Molecular ion characterization of this trimetallic complex is desired. If the molecular ion cannot be produced, a better knowledge of some limitations will be obtained, with hopes of subsequent LI-TOF-MS improvements in the analysis of these organometallic complexes. Since successful structural characterization depends on a complete knowledge of all aspects of the LI-TOF-MS process, sample preparation, mechanisms of ionization, and fragmentation patterns of the analyte must be understood. Analyses of samples related to the heteronuclear trimetallic complex will be performed to aid in understanding the processes that occur in complicated coordination compounds.

VI.4-- SAMPLES ANALYZED

Three different organometallic compounds, synthesized at VPI&SU by the research group lead by Dr. Karen Brewer, were investigated. The target sample, a trimetallic heteronuclear compound, $\{[(bpy)_2Ru(dpp)]_2IrCl_2\}(PF_6)_5$ (abbreviated "JSB"; see Figure VI.1), was the most complex of the three, and the subsequent analytes were chosen to more thoroughly study the fragmentation and ionization processes which were observed in the $\{[(bpy)_2Ru(dpp)]_2IrCl_2\}(PF_6)_5$ complex. A much simpler, single-metallic species, $[Ir(dpp)_2Cl_2](PF_6)$ (abbreviated "Dbl-Ir"; see Figure VI.2), assessed iridium ionization processes and how the LI-TOF-MS and MALDI perform with a lower molecular weight organometallic complex. A homonuclear trimetallic species, $\{[(bpy)_2Ru(dpp)]_2RuCl_2\}(PF_6)_4$ (abbreviated "Tri-Ru"; see Figure VI.3), probed the bond strengths and potential competition between the metals of the $\{[(bpy)_2Ru(dpp)]_2IrCl_2\}(PF_6)_5$ complex for the bridging ligands, and was used to confirm peak assignments in the spectra. In addition, since both the $\{[(bpy)_2Ru(dpp)]_2RuCl_2\}(PF_6)_4$ and the $\{[(bpy)_2Ru(dpp)]_2IrCl_2\}(PF_6)_5$ compounds contain three metal atoms, a comparison of the two complexes addressed the fragility of the heteronuclear $\{[(bpy)_2Ru(dpp)]_2IrCl_2\}(PF_6)_5$ versus the homonuclear $\{[(bpy)_2Ru(dpp)]_2RuCl_2\}(PF_6)_4$. The masses of the molecular ions (M^+) and pseudomolecular ions (PM^+; the species with the counterions removed) for each of the three complexes are listed in Table VI.1.

Table VI. 1: Theoretical molecular masses and pseudomolecular masses of the three organometallics studied.

$\{[(bpy)_2Ru(dpp)]_2IrCl_2\}(PF_6)_5$ "JSB"	
SPECIES	**M/Z**
Molecular ion (M^+)	2283
Pseudomolecular ion (PM^+) $[(M^+-(PF_6)_5]$	1559

$Ir(dpp)_2Cl_2(PF_6)$ "Dbl-Ir"	
SPECIES	**M/Z**
Molecular ion (M^+)	876
Pseudomolecular ion (PM^+) $[(M^+-(PF_6)]$	731

$\{[(bpy)_2Ru_(dpp)]_2RuCl_2\}(PF_6)_4$ "Tri-Ru"	
SPECIES	**M/Z**
Molecular ion (M^+)	2048
Pseudomolecular ion (PM^+) $[(M^+-(PF_6)_4]$	1468

$\{[(bpy)_2Ru(dpp)]_2IrCl_2\}\ (PF_6)_5$

"JSB"

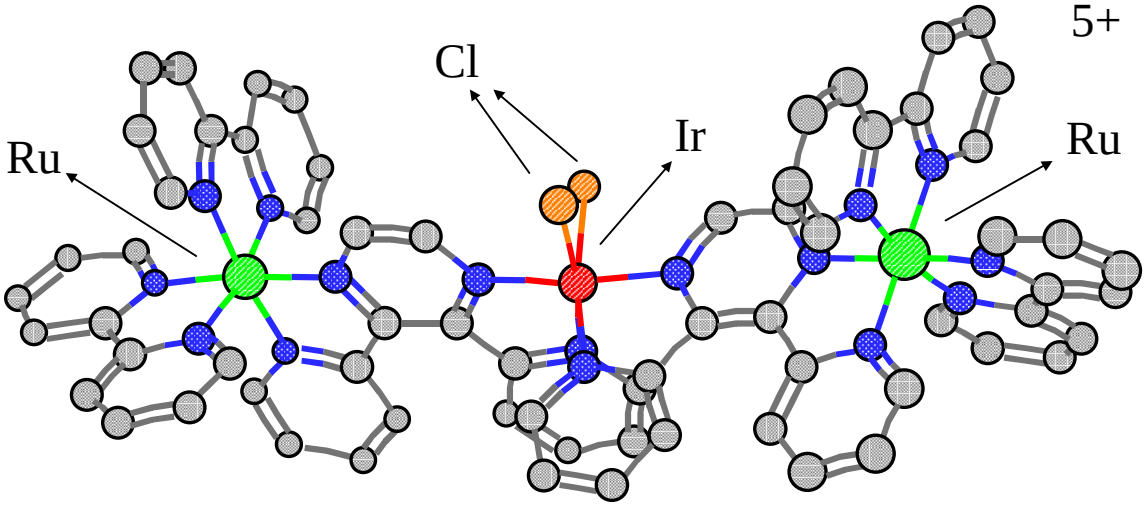

Figure VI. 1: Schematic of the heteronuclear trimetallic complex $\{[(bpy)_2Ru(dpp)]_2IrCl_2\}(PF_6)_5$ ("JSB").

$[Ir(dpp)_2Cl_2]$ (PF_6)

“Dbl-Ir”

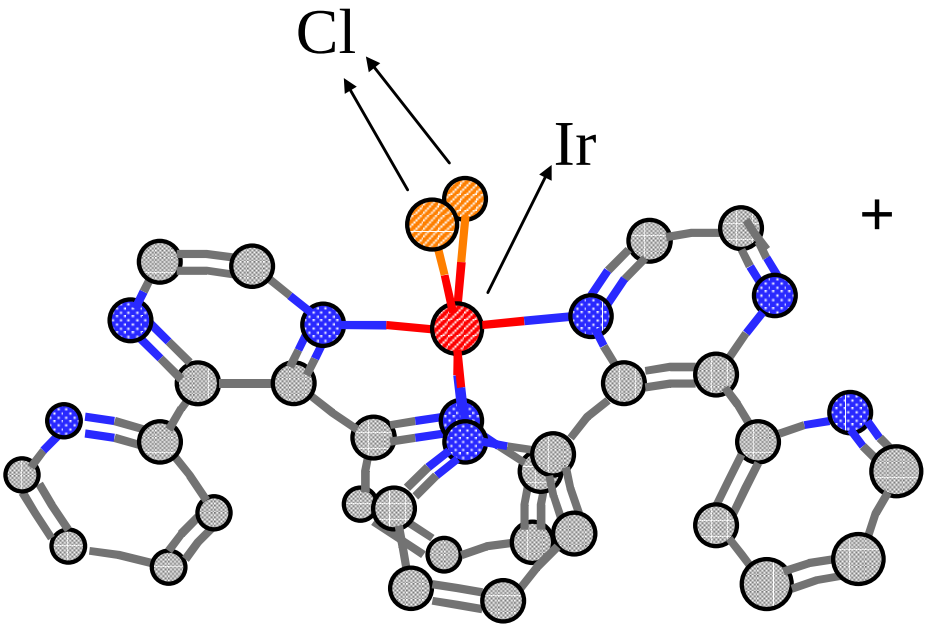

Figure VI. 2: Schematic of the monometallic complex $[Ir(dpp)_2Cl_2](PF_6)$ ("Dbl-Ir").

$\{[(bpy)_2Ru(dpp)]_2RuCl_2\}\ (PF_6)_4$

"Tri-Ru"

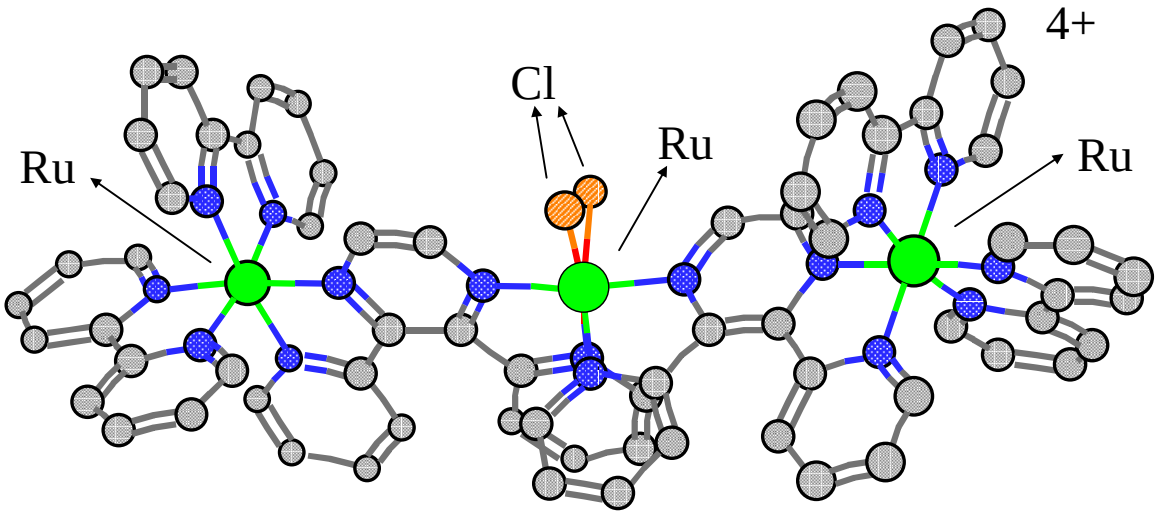

Figure VI. 3: Schematic of the homonuclear, trimetallic complex $\{[(bpy)_2Ru(dpp)]_2RuCl_2\}(PF_6)_4$ ("Tri-Ru").

VI.5-- INSTRUMENTAL PARAMETERS

The 355-nm laser beam from the Nd^{3+}:YAG was again used for sample ablation. The beam was focused into the sample "cup"—a 1/16-inch deep, 5/32-inch diameter depression in an aluminum disk—through a 25-cm focal length lens to create a beam radius on the sample of ~11 μm. In addition, for "defocused" analyses, the lens was raised 0.6 cm from the focused position to increase the laser spot radius by approximately a factor of five. Repeller delays between 6 μs and 70 μs were used to search for a range of mass signals that could be detected. In general, repeller delays from 20 μs to 50 μs generated mass spectra of the most abundant ions. Laser energies were selected from ~4 μJ to ~50 μJ to generate appreciable ion yields without saturating the detector. Resolution of at least 350 ($t/2\Delta t_{FWHM}$) was achieved in most spectra. Unless otherwise noted, 25 laser shots were averaged to acquire a spectrum.

VI.6-- LASER BEAM DEFOCUSING AND SIGNAL AVERAGING

To improve the S/N ratio and possibly observe high molecular mass ions from background noise, the effects of increasing the number of laser shots averaged per spectrum and laser beam defocusing were studied. Investigations with the $\{[(bpy)_2Ru(dpp)]_2RuCl_2\}(PF_6)_4$ compound revealed a distinct relation between the sample preparation procedure and the effects of signal averaging. Increasing the number of laser shots averaged per spectrum, as was discussed in chapter II, improves the S/N ratio of the spectrum. With the thinly deposited MALDI samples, however, the signal deteriorated rapidly as the laser quickly removed the fine crystals. Averaging twenty-five laser shots did not greatly diminish the peak intensities, which is slightly better than the usual 10 laser shots that most MALDI techniques employ[90]. The MALDI matrix influenced the rate of signal decay, as intensities from the thin DHB crystals decreased faster than from the dense DHC crystals. Furthermore, for directly depositied samples, spectra could be compiled from the average of up to 75 laser shots.

The laser beam focus highly affects the energy deposited per unit area of the sample. With a minimal focused beam spot radius of ~11 μm, a laser energy of 20 μJ corresponds to energy densities of ~0.17 $\mu J/\mu m^2$. By raising the lens height by 0.6 cm,

the beam becomes "defocused" by approximately a factor of 5 according to the beam waist calculation (Equation IV.1)[96]:

$$w(z) = w_0[1+\left(\frac{\lambda z}{\pi w_0^{\,2}}\right]^{1/2}$$

Equation VI. 1: Beam waist (radius) calculation for a defocused beam.

where z is the displacement in lens height from the focal position, w_0 is the beam radius when focused, and w_z is the beam radius at the lens height z.

With this in mind, we sought to create even "softer" ablation conditions to remove the analyte intact into the gas phase. The defocused beam energy density is thus ~ 0.007 $\mu J/\mu m^2$, and, theoretically, the defocused energy density will decrease by about 25 times compared to the focused beam. The defocused-beam spectra, however, did not reveal any different, larger portions of the molecule. One important advantage of the defocused beam was the increased number of laser shots that could be averaged per spectrum before the signal decreased. As an example, up to 100 laser shots could be averaged versus only 25 for the defocused and focused beam conditions, respectively, for DHC-prepared samples. This improved the S/N ratio in many spectra.

VI.7-- MATRIX SELECTION FOR MALDI AND SAMPLE PREPARATION

Sample preparation fell into two categories: (i) direct laser ablation and (ii) MALDI. For direct laser ablation analyses, a concentrated solution of the organometallic complex in a volatile solvent (acetone, ethanol, or acetonitrile) was prepared. The solution was deposited slowly into the sample "cup" (~3 μL to 7μL total volume in 1-μL increments) which was then attached to the sample probe. Following evaporation, a dense film of the analyte covered the surface, and the probe was inserted into the mass spectrometer.

[96] W. Demtroder. *Laser Spectroscopy—Basic Concepts and Instrumentation.* Vol. 5 in the Springer Series in Chemical Physics. New York: Springer-Verlag, 1982.

Most of the matrices for our MALDI studies are traditional MALDI matrices that have been successful in protein analyses. Substituted benzoic acid derivatives [(2,5-dihydroxybenzoic acid "DHB")] and cinnamic acid derivatives [(3,4-dihydroxycinnamic acid ("DHC") and 3,5-Dimethoxy-4-hydroxycinnamic acid ("Sinapinic acid")] are polar, soluble in most polar organic solvents, and able to donate a proton to the analyte for ionization. A non-traditional matrix that has been used effectively in polymer analyses, 9-nitroanthracene, was also employed. This non-polar matrix is soluble in acetone, but does not have an available H^+, making proton transfer from the matrix impossible and promoting ionization by radical formation.

A variety of MALDI conditions were employed. A matrix solution (~20 mg/ml to 60 mg/ml) in a volatile solvent (acetone, ethanol, acetonitrile) was first prepared. A solution of the analyte in the same solvent (~2 mg/ml) was also prepared. Appropriate quantities of each solution were combined in 1:50 to 1:1000 ratios of analyte:matrix for the sample solution. Approximately 6 μL of the sample solution was deposited into the sample cup in 1-μL increments. After evaporation, crystals of the analyte and matrix covered the surface. Visual assessment of the thickness of the sample dictated the amount of sample deposited. Co-crystallization of the analyte and matrix was also assessed visually by depositing 1 μL of the sample solution onto a bare aluminum disk and observing the crystals which formed following solvent evaporation.

VI.8-- $[Ir(dpp)_2Cl_2](PF_6)$ ("Dbl-Ir") RESULTS

Analysis of the relatively simple, single-metallic complex $[Ir(dpp)_2Cl_2](PF_6)$ addresses the applicability of TOF-MS and MALDI for small inorganic complexes. Also, assessing the ionization of Ir-containing species and comparing $[Ir(dpp)_2Cl_2](PF_6)$ spectra with $\{[(bpy)_2Ru(dpp)]_2IrCl_2\}(PF_6)_5$ spectra improves interpretations of the heteronucluear trimetallic $\{[(bpy)_2Ru(dpp)]_2IrCl_2\}(PF_6)_5$ spectra. The production of the molecular ion from this smaller $[Ir(dpp)_2Cl_2](PF_6)$ species (molecular weight 876 amu) and structural characterization were sought. The analysis of both direct laser desorption (no matrix) and MALDI samples tests the applicability of matrix-assisted techniques for inorganic species.

VI.8.1-- Straight Ablation

The sample was first laser-ablated directly without a matrix. Acetone readily dissolved the $[Ir(dpp)_2Cl_2](PF_6)$ sample, and a concentrated solution was prepared. Several microliters were deposited into the sample cup, and a thick sample formed as the acetone evaporated.

The direct ablation sample yielded abundant signals throughout the mass range from ~100 amu to 800 amu. As with previous samples, irradiating a "fresh" spot generated more intense signals than sampling from a previously ablated area. The threshold laser energies necessary for ionization were approximately 4 μJ to 5 μJ.

A complete summary of the ions observed is presented in Table VI.2. Although straight ablation of the complex failed to produce the molecular ion (m/z = 876) consistently, the pseudomolecular ion (PM^+) (~733 amu) was produced in most spectra at a S/N ratio of at least 4, depending on the laser energy and TOF-MS conditions (repeller delay). Successive chloride losses from the pseudomolecular ion are shown by abundant signals at ~696 amu $(PM - Cl)^+$ and ~660 amu $(PM - Cl_2)^+$. These high-mass species may be important for structural identification, as the $Ir(dpp)_2$ backbone (660 amu) is confirmed.

Fragmentation of the directly deposited sample was high, as complete cleavage of one dpp ligand off of $Ir(dpp)_2$ produced $Ir(dpp)^+$ (~425 amu). Also, removal of one of the bidentate nitrogen bonds of a single dpp ligand yielded abundant peaks at ~503 amu and ~580 amu, which correspond to various losses from the ligand. In spectra that were optimized specifically for the lower-mass region (under 300 amu), a variety of fragments were observed. The excellent resolution on the ligand peak (234 amu) reveals electron abstraction as the mode of ionization, since proton transfer would generate peaks at 235 amu instead of 234 amu. The bare metal ion Ir^+ was not observed for any laser energy, but high-energy (over ~30 μJ) ablation produced PF_4^+ from the counterion.

The relation between the laser energy and the fragmentation of the pseudomolecular ion was studied. In general, increases in the energy of ablation removed chloride ions readily and fragmented the dpp ligand. A comparison of the representative spectra of three laser energies (see Figures VI.4, VI.5, and VI.6) highlights this finding. All of these spectra were obtained with the same TOF-MS

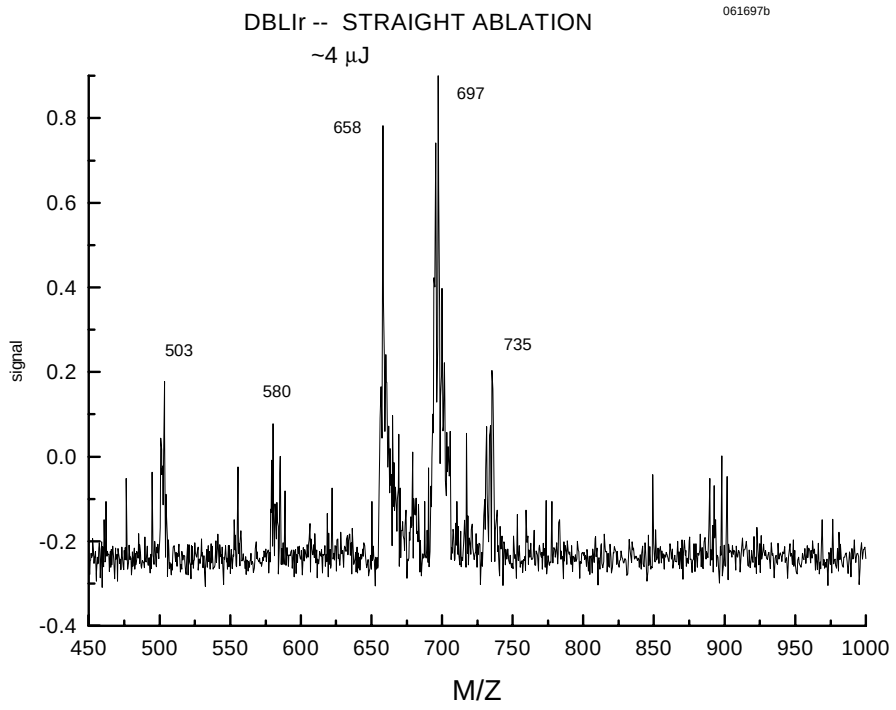

Figure VI. 4: $[Ir(dpp)_2Cl_2](PF_6)$ ("Dbl-Ir"); Spectrum obtained for 4 μJ ablation energy of a straight ablation sample.

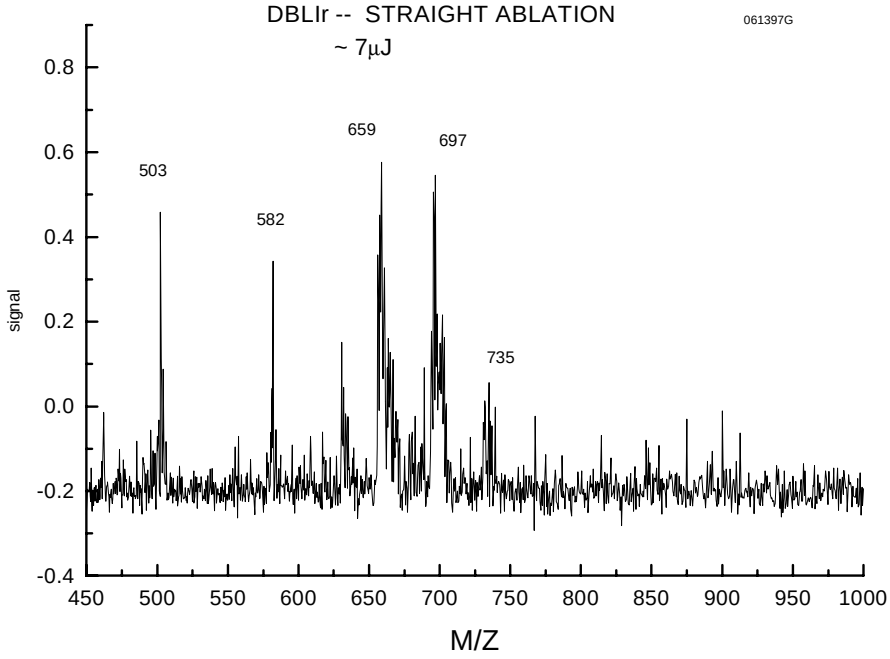

Figure VI. 5: $[Ir(dpp)_2Cl_2](PF_6)$ ("Dbl-Ir"); Spectrum obtained with 7 μJ ablation energy of a straight ablation sample.

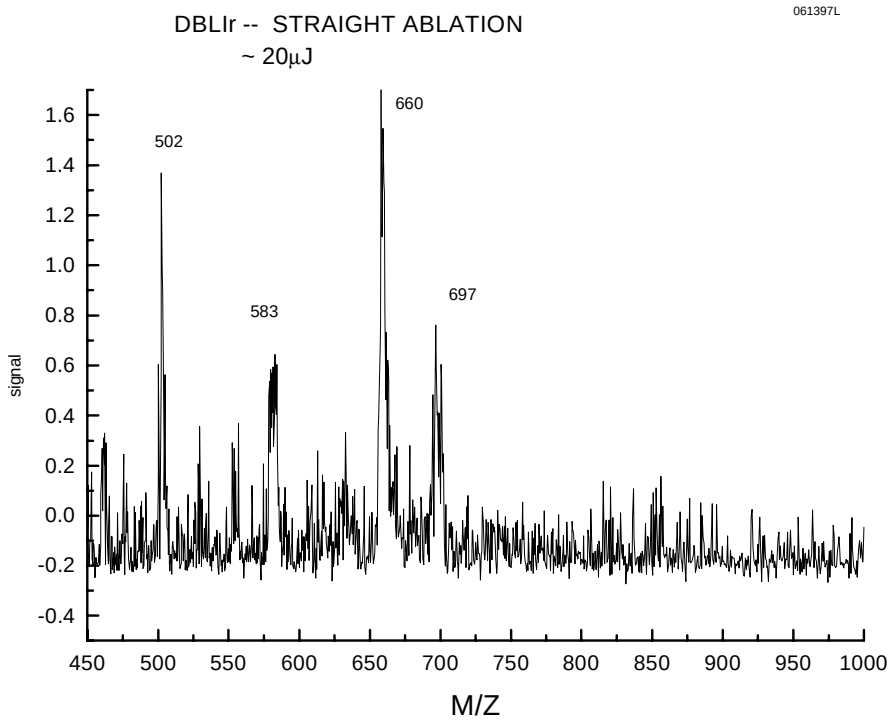

Figure VI. 6: $[Ir(dpp)_2Cl_2](PF_6)$ ("Dbl-Ir"); Spectrum obtained with 20 μJ ablation energy of a straight ablation sample.

conditions (optimized for the ~400 to 1000 amu region) at laser energies of ~4 μJ, ~7 μJ, and ~20 μJ, respectively. Comparing the three spectra, the ratio of the pseudomolecular ion to single- and double-chloride losses clearly decreases as the laser energy is increased. In fact, the highest laser energy generates (~20 μJ) little of the pseudomolecular ion at all, and the loss of both chloride ions $(PM - Cl_2)^+$ yields a very intense peak at ~660 amu.

VI.8.2-- $[Ir(dpp)_2Cl_2](PF_6)$ in 2,5-dihydroxybenzoic acid (DHB) matrix

Although the production of the pseudomolecular ion in the straight ablation sample was important, MALDI was applied to the complex to reduce fragmentation, increase the S/N ratio, and hopefully reveal the intact molecular ion. The first matrix employed, 2,5-dihydroxybenzoic acid, was chosen based on the successful results with the $\{[(bpy)_2Ru(dpp)]_2IrCl_2\}(PF_6)_5$ compound. Samples of the analyte/matrix mixture were investigated for two different solvents, ethanol and acetone, at an analyte:matrix ratio of approximately 1:100. The quickly-evaporating acetone sample appeared to yield slightly thicker crystals upon visual inspection. In both cases, at least 7 μL of the sample were applied to the sample cup to obtain a substantial sample for laser ablation.

The major ion peaks generated in the MALDI samples of the $[Ir(dpp)_2Cl_2](PF_6)$ complex are highlighted in Table VI.2, and a typical spectrum of the analyte prepared with DHB in acetone (TOF-MS conditions optimized for the mass range ~400-1000 amu) is shown in Figure VI.7. Most notably, there is less fragmentation in the MALDI spectra than in direct-ablation spectra. Specifically, the lack of fragmentation of the dpp ligand is revealed by the low intensities of the peaks at ~503 amu and ~580 amu. The pseudomolecular ion is present in enhanced yields for laser energies up to ~35 μJ, which is also a major accomplishment from the straight-ablation spectra. In fact, the high-mass region dominated most spectra, with high intensities of the pseudomolecular ion as well as successive losses of chloride from the pseudomolecular ion. Absent in these spectra, however, is the complete molecular ion with the counterion intact.

Slightly less successful results were obtained with the MALDI sample prepared with DHB in ethanol. Although the matrix did reduce fragmentation, yields of the

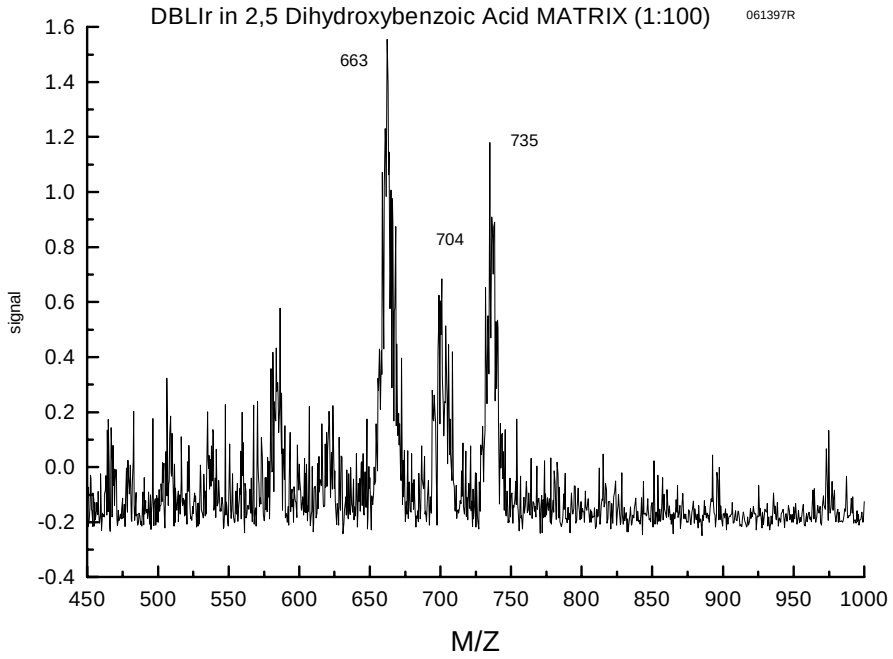

Figure VI. 7: $[Ir(dpp)_2Cl_2](PF_6)$ ("Dbl-Ir"); MALDI spectrum of a sample prepared in DHB matrix (TOF-MS optimized for ~400-1000 amu region).

pseudomolecular ion were less than when acetone was the solvent. Furthermore, samples prepared from ethanol appeared more highly affected by laser energy increases, although not quite as dramatically as the straight ablation sample. One possibility is poor co-crystallization of the analyte and the matrix. This inhomogeneity would account for the similarities in the observed spectra and laser energy influences of the straight ablation and ethanol-deposited samples.

The mechanism of ionization for the MALDI samples in 2,5-dihydroxybenzoic acid can be assessed using the dpp ion peak (235 amu). In contrast to the signal in the straight ablation sample (234 amu), the MALDI technique protonated the ligand to induce ionization, as revealed by the $(dpp + H)^+$ signal one mass unit higher than the bare dpp ligand ionized by electron abstraction.

VI.8.3-- $[Ir(dpp)_2Cl_2](PF_6)$ in 3,4-dihydroxycinnamic acid (DHC) matrix

MALDI was again attempted with a different matrix under similar conditions as were employed with the DHB sample. Samples prepared with 3,4-dihydroxycinnamic

acid again used a 1:100 analyte:matrix ratio with acetone as the solvent. This matrix is significantly less soluble in acetone than DHB, and formed large, thick crystals as the solvent evaporated. Only 4 μL were deposited into the sample cup because of the thickness of the sample crystals.

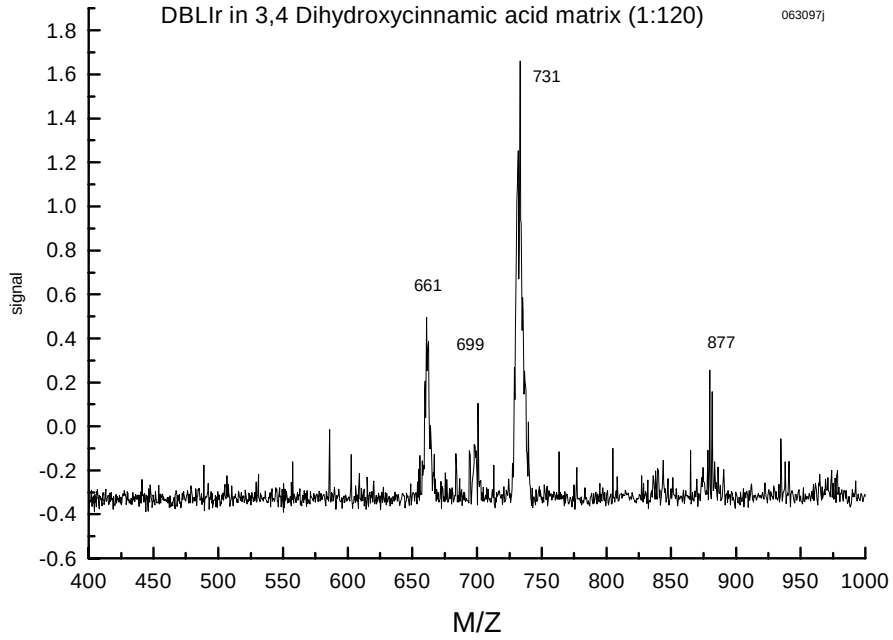

Figure VI. 8: $[Ir(dpp)_2Cl_2](PF_6)$ ("Dbl-Ir"); MALDI spectrum of a sample prepared in DHC matrix (TOF-MS optimized for ~400-1000 amu region).

Excellent results were obtained with the MALDI spectra using the DHC matrix. Most importantly, the molecular ion (~876 amu) was consistently generated at S/N ratios of at least 5 in spectra optimized for the high-mass ions, as is shown in Figure VI.8. In addition, the intensities of the pseudomolecular ion and the $(PM - Cl)^+$ and $(PM - Cl_2)^+$ moieties were enhanced over any fragmentation peaks, and background noise was minimized. It is interesting to note that the ion peak resulting from the loss of a single chloride ion $(PM - Cl)^+$ is less intense than either the pseudomolecular ion (~731 amu) or the chloride-free $Ir(dpp)_2{}^+$ species (~660 amu). When fragmentation was desired, the laser energy could be increased to approximately 40 μJ without the loss of these

pseudomolecular ion peaks, and the most common species including the observed fragment ions are listed in Table VI.2. The role of the matrix to absorb the energy from the laser pulse is most clearly portrayed by the lack of dissociation of the dpp ligands (i.e. little signal for ~503 and ~580 amu).

Significant conclusions for the mode of ionization can be obtained from the MALDI results using 3,4-dihydroxycinnamic acid. As with the sample prepared with 2,5- Dihydroxybenzoic acid as the matrix, proton transfer seems a prominent form of ionization, as the dpp peak (specifically, dpp + H)$^+$ again appears at 235 amu. The exact mechanism of ionization of the other ion peaks could not be ascertained from either the straight-ablation or matrix samples due to the complexity of the isotopic distributions. Since the pseudomolecular ion naturally carries a positive charge, the matrix is not needed for the formation of the positive ion. However, because the molecular ion was observed in the samples prepared from DHC, the matrix most likely donated a proton to ionize the complete, intact $[Ir(dpp)_2Cl_2](PF_6)$ molecule.

Overall, the MALDI samples of $[Ir(dpp)_2Cl_2](PF_6)$ prepared with DHC yielded tremendous results and high-quality spectra. The observation of the molecular ion, pseudomolecular ion, and chloride losses confirm the structure of the molecule. The dpp ligand was generated through selective fragmentation by using high laser energies. Furthermore, electron abstraction was responsible for ionization of the straight ablation sample, whereas proton transfer was the ionization mechanism for MALDI samples.

VI.8.4-- Discussion

Several questions were answered after analyzing the $[Ir(dpp)_2Cl_2](PF_6)$ species. Although this is only a single-metal species, the ability to detect the molecular ion is significant, and success in this aspect highlights the potential of MALDI for the characterization of organometallic complexes in their intact forms. In addition, for rapid characterization of the species, the directly-deposited sample revealed the pseudomolecular ion, so extensive trial-and-error approaches for matrix selection are not necessary to produce this ion. On the other hand, the matrix was crucial for improving the S/N ratio and reducing fragmentation of the compound. Since there seems to be no

problems in ionizing an iridium-containing species, fragments containing Ir should be expected in the $\{[(bpy)_2Ru(dpp)]_2IrCl_2\}(PF_6)_5$ spectra.

The differences in the spectra of the various MALDI matrices used with the $[Ir(dpp)_2Cl_2](PF_6)$ sample reveals the importance of finding a suitable matrix-analyte combination. The optimum results were obtained with the 3,4-dihydroxycinnamic acid matrix, while the 2,5-dihydroxybenzoic matrix was less successful. Furthermore, the influence of the solvent and co-crystallization of the analyte with the matrix was revealed through the poor results of samples prepared in the DHB matrix using ethanol compared to acetone. Co-crystallization appears an essential factor again, as the noticeably "thick" DHC crystals produced the most favorable spectra.

Table VI. 2: Summary of the ions observed in the analysis of the $[Ir(dpp)_2Cl_2](PF_6)$ ("Dbl-Ir") complex.

$[Ir(dpp)_2Cl_2](PF_6)$ ("Dbl-Ir") RESULTS

DIRECT ABLATION	Dbl-Ir in 2,5 DHB matrix	Dbl-Ir in 3,4 DHC matrix
107	--	--
110-210 {fragments}	--	--
234	235	235
~425	~425	~425
~503	-	-
~580	~580(small)	~580(small)
~661	~661	~661
~698	~698	~698
~733	~733	~733
--	~850(small)	
--	--	~877
--	~968(small)	~968(small)

PROBABLE IDENTIFICATIONS OF THE MAJOR ION PEAKS

MASS (amu)	STRUCTURE	
107	PF_4^+	
234/235	dpp^+ / $(dpp + H)^+$	
~425	$Ir(dpp)^+$	
~503	$[Ir(dpp) + \text{fragment of dpp}]^+$	
~580	$[Ir(dpp) + \text{fragment of dpp}]^+$	
~662	$(PM - Cl_2)^+$	$Ir(dpp)_2$
~698	$(PM - Cl)^+$	$Ir(dpp)_2Cl^+$
~733	PM^+	$Ir(dpp)_2Cl_2^+$
~876	M^+	$Ir(dpp)_2Cl_2(PF_6)_4^+$

VI.9-- $\{[(bpy)_2Ru(dpp)]_2RuCl_2\}(PF_6)_4$ ("Tri-Ru") RESULTS

Analysis of the $\{[(bpy)_2Ru(dpp)]_2RuCl_2\}(PF_6)_4$ compound provides information on the relative fragility of the Ir-dpp and Ru-dpp bonds and improves the interpretation of mass spectra of the $\{[(bpy)_2Ru(dpp)]_2IrCl_2\}(PF_6)_5$ compound. A major question to be addressed is "can MALDI produce larger fragments (and possibly the molecular ion) from a homonuclear trimetallic compound such as $\{[(bpy)_2Ru(dpp)]_2RuCl_2\}(PF_6)_4$ versus a heteronuclear trimetallic such as $\{[(bpy)_2Ru(dpp)]_2IrCl_2\}(PF_6)_5$?". Again, several matrices and solvents will be investigated and the results compared.

VI.9.1-- Straight Ablation

Acetone and acetonitrile were used as deposition solvents for the direct laser ablation samples of the $\{[(bpy)_2Ru(dpp)]_2RuCl_2\}(PF_6)_4$ complex. The complex is highly soluble in both solvents, and a separate sample of each was prepared. The role of the deposition solvent seems unimportant, as mass spectral results were similar for both sample preparation conditions.

Laser ablation of the directly deposited sample produced a variety of fragment ions (see Table VI.3 and Figure VI.9), but the molecular ion could not be detected. Threshold laser energies for ion production (~3 μJ) fragmented the complex to produce bpy and dpp ligand ions (157 amu and 234 amu). These energies also yielded ion signals from a single ruthenium atom bonded to a single ligand (Ru(bpy) ~257 amu, and(Ru(dpp) ~334 amu), as well as a single ruthenium atom bonded to one of each ligand (~490 amu) or to two bpy ligands (~414 amu). Slight increases in the laser energy greatly intensified the overall signal from the ligand ions and produced larger fragments of the molecule, $(bpy)_2Ru(dpp)^+$ (~647 amu) and $Ru(dpp)_2^+$ (~570 amu). These species were the largest portions of the molecule that were detected. Further ablation energy increases (over ~15 μJ) extensively fragmented the $\{[(bpy)_2Ru(dpp)]_2RuCl_2\}(PF_6)_4$ and ligand dissociation products dominated the low-mass region of the spectrum. With laser energies over ~25 μJ, the bare Ru^+ isotopes and a dissociation product of the counterion (PF_4^+) were detected. For all ablation energies, the most intense peaks were $Ru(bpy)_2^+$ (~414 amu) and $(bpy)Ru(dpp)^+$ (~490 amu).

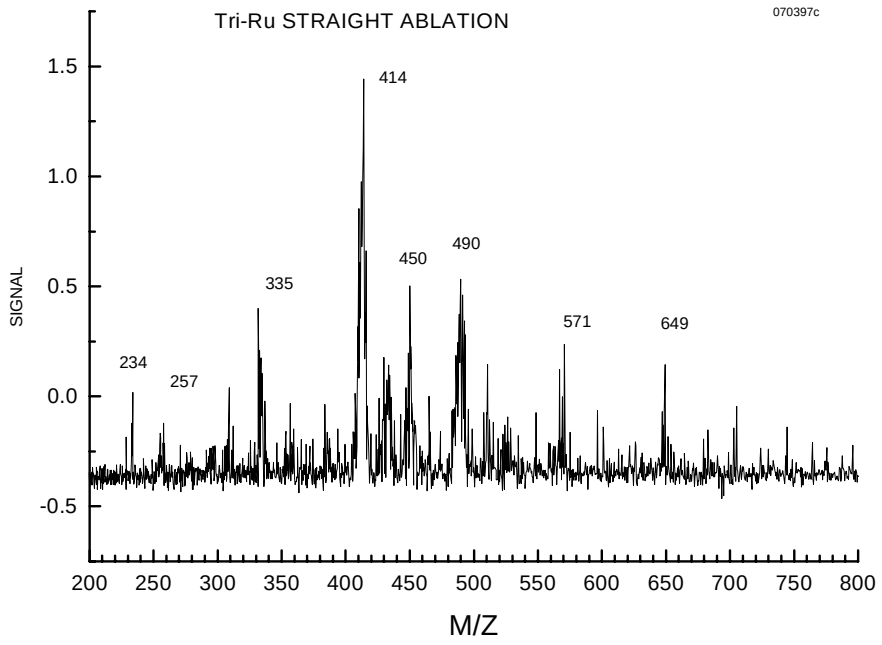

Figure VI. 9: $\{[(bpy)_2Ru(dpp)]_2RuCl_2\}(PF_6)_4$ ("Tri-Ru"); Typical spectrum of a directly ablated sample TOF-MS optimzed for ~200-700 region.)

The quality of the mass spectra of the directly-deposited samples was low. Complicated spectra resulted from extensive fragmentation of the molecule, making data interpretation difficult. Also, high noise levels reduced the S/N ratio throughout the mass region.

VI.9.2-- $\{[(bpy)_2Ru(dpp)]_2RuCl_2\}(PF_6)_4$ in 2,5- Dihydroxybenzoic acid (DHB) matrix

MALDI using the DHB matrix significantly improved the mass spectra of the tri-ruthenium compound. Samples were prepared in two different solvents, acetonitrile and acetone, at analyte:matrix ratios of approximately 1:100. Upon visual inspection, the crystals appeared long and thin, and the spectra of the samples were nearly identical.

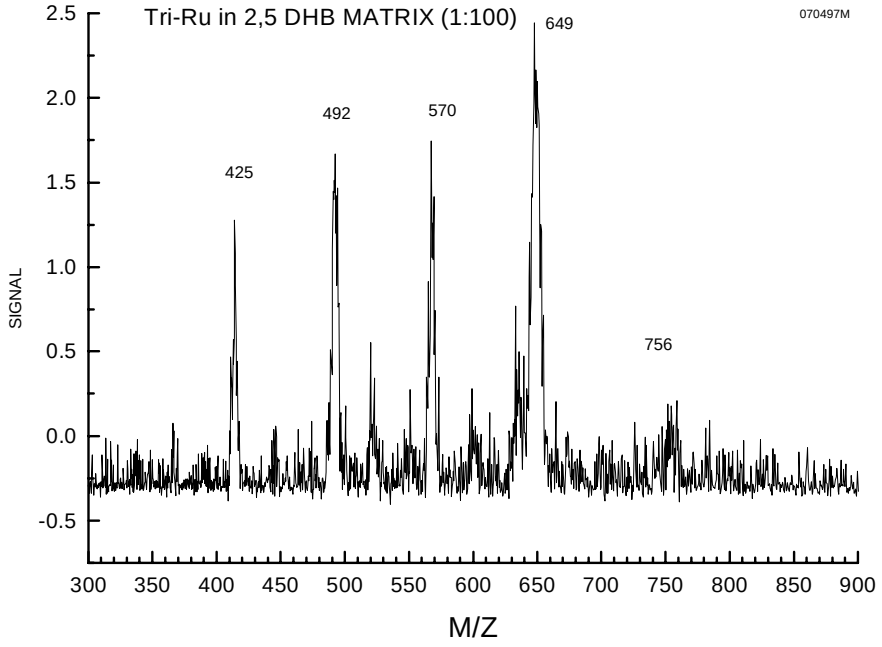

Figure VI. 10: $\{[(bpy)_2Ru(dpp)]_2RuCl_2\}(PF_6)_4$ ("Tri-Ru"); MALDI spectrum of a sample prepared in DHB matrix with acetone solvent (TOF-MS optimized for ~300-800 amu region)

The matrix-assisted technique produced spectra that were easier to interpret, with less fragmentation and a higher S/N ratio in comparison to the straight ablation sample. A typical $\{[(bpy)_2Ru(dpp)]_2RuCl_2\}(PF_6)_4$ MALDI spectrum using the DHB matrix with acetone as the solvent, optimized for the mass region 300-800 amu (see Figure VI.10), portrays the most common ions observed in this region, and Table VI.3 contains a complete list of the major ions. Comparing the MALDI results with straight ablation, there was a significant increase in the ion yield of the large fragment $(bpy)_2Ru(dpp)^+$ (~647 amu) when the matrix was employed. In addition, an even larger fragment of the complex was successfully detected at ~750 amu (in most cases with at least S/N ~3), corresponding to the retention of the central ruthenium atom with the bridging dpp ligand and complete ruthenium side unit $[(bpy)_2Ru(dpp)Ru]^+$. The major fragment ions, including this large species, were observed at threshold laser energies (~6 μJ), and higher laser energies did not ionize larger fragments of the molecule. The range of laser

energies usable was up to ~50 μJ before ion signals from the matrix dominated the spectra.

In general, spectra of the 1:100 samples prepared from acetone and acetonitrile were nearly identical. The sample prepared from acetonitrile, however, produced a slightly larger abundance of the largest fragment $[(bpy)_2Ru(dpp)Ru]^+$, and a typical spectrum is shown in Figure VI.11. With the acetonitrile solvent, a lower analyte concentration (1:1000 dilution in the matrix) was also attempted. This concentration proved too low to generate significant analyte ion yields. In fact, finding a crystal to provide good signal intensities was tedious. Even when ablating a "good spot", the signal intensity decreased drastically for averaging even 25 laser shots.

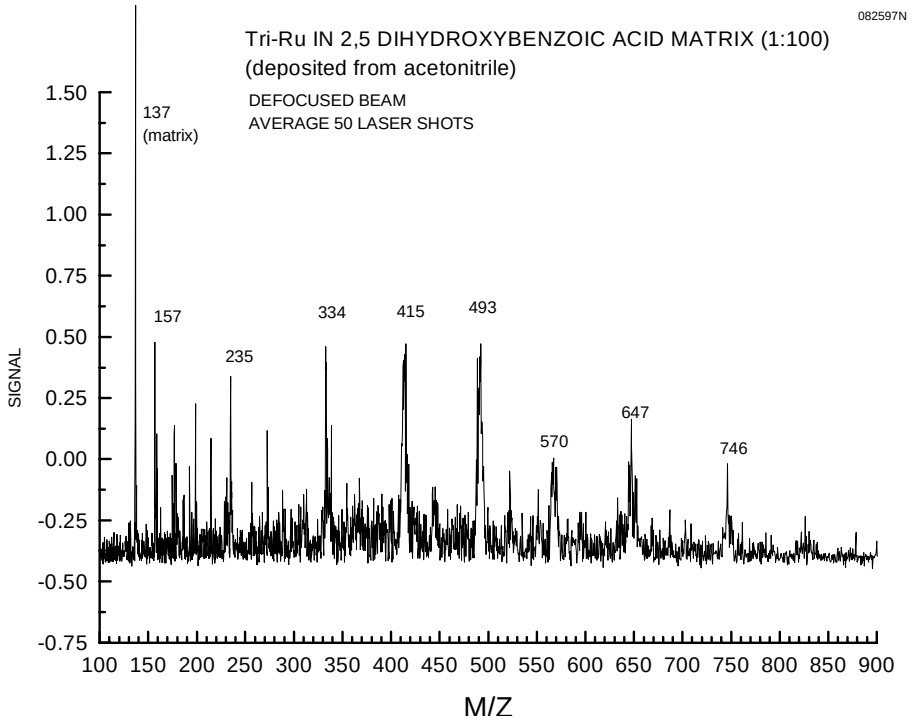

Figure VI. 11: $\{[(bpy)_2Ru(dpp)]_2RuCl_2\}(PF_6)_4$ ("Tri-Ru"); MALDI spectrum of a sample prepared in DHB with acetonitrile solvent (TOF-MS optimized for ~300-800 amu region).

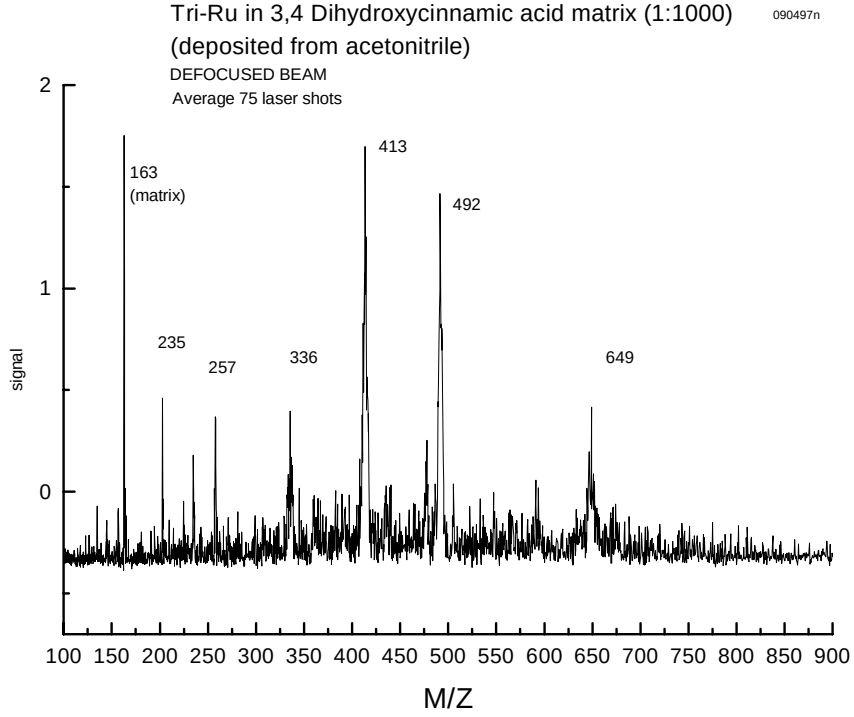

Figure VI. 12: $\{[(bpy)_2Ru(dpp)]_2RuCl_2\}(PF_6)_4$ ("Tri-Ru"); MALDI spectrum of a sample prepared in DHC matrix (TOF-MS optimized for ~200-700 amu region).

VI.9.3-- $\{[(bpy)_2Ru(dpp)]_2RuCl_2\}(PF_6)_4$ in 3,4-dihydroxycinnamic acid (DHC) matrix

Compared to the direct laser ablation of $\{[(bpy)_2Ru(dpp)]_2RuCl_2\}(PF_6)_4$, MALDI using DHC as the matrix improved the mass spectra. As with the DHB matrix, acetone and acetonitrile were investigated as solvents for sample preparation. The DHC matrix is not as soluble in either of these solvents as DHB, and the resulting crystallization of the matrix and $\{[(bpy)_2Ru(dpp)]_2RuCl_2\}(PF_6)_4$ produced thicker, denser crystals after evaporation. Consequently, only a few microliters were deposited into the sample cup to form a dense film of crystals.

Compared to direct laser ablation, the sample prepared in the DHC matrix exhibited cleaner spectra with enhanced ion yields from the larger fragments, $Ru(bpy)_2^+$ (~414 amu), $(bpy)Ru(dpp)^+$ (~492 amu), and $(bpy)_2Ru(dpp)^+$ (~647 amu). Similar to the DHB matrix, the choice of solvent (acetone or acetonitrile) had little effect on the observed crystallization or mass spectra, and the major ions are listed in Table VI.3. A common spectrum, optimized for the 200-700 amu mass region (see Figure VI.12), shows the high quality of the spectra with this matrix; S/N ratios are increased even over the samples prepared in DHB.

Although most of the main peaks obtained by the ablation of the DHC-prepared sample are the same as the DHB-prepared sample, several important differences must be noted. Crystallization was drastically different for the two matrices. The wispy, elongated crystals of the sample in DHB produced only a thin deposit in the sample cup, while the DHC matrix co-crystallized with the sample as a thick, densely packed film of crystals. The effect of the thicker sample (although the analyte:matrix ratio in both cases was 1:100) impacted the number of laser shots that could be averaged per spectrum. For the DHC matrix, spectra could be averaged for up to 75 laser shots before the signal substantially decreased. Thus, the background noise in the spectra was diminished without significantly reducing the intensity of the important fragment ions. In addition, even the low-concentration (1:1000) sample produced quality mass spectra with 75 laser

shot averaging capabilities. In general, finding a well-formed crystal for laser ablation was easier.

In mass spectral results, the DHC matrix did not generate the large fragment $[(bpy)_2Ru(dpp)Ru]^+$ (~750 amu) that was observed in the DHB-prepared samples. Also, the peaks at ~570 amu $[Ru(dpp)_2^+]$ and ~334 amu $[Ru(dpp)]^+$ were detected in decreased abundance compared to the DHB-prepared spectra. A possible explanation for the latter observation could be selective ionization following fragmentation of the complex to produce high yields of $Ru(bpy)_2^+$ and $(bpy)Ru(dpp)^+$ with losses of *neutral* Ru(dpp) and $Ru(dpp)_2$. This would account for the enhancement of the peaks at ~414 amu and ~492 amu with the concurrent decrease in the peaks at ~334 amu and ~570 amu.

VI.9.4-- Discussion

Although several sample preparation conditions were used, the molecular or pseudomolecular ions could not be produced in the mass spectra of the tri-ruthenium complex. In particular, straight ablation produced extensive fragmentation. For both the DHB and DHC matrices, MALDI proved invaluable for improving the S/N ratio of the spectra and intensifying the yield of larger fragments of the molecule. Specifically, the $[(bpy)_2Ru(dpp)]^+$ fragment (~647 amu), a complete side unit of the molecule, exhibited enhanced stability in both matrices. Furthermore, MALDI allowed simpler ion peak identification with a reduction in small fragments of the molecule. A significant accomplishment was achieved with the DHB matrix, as a moiety containing two ruthenium atoms $[(bpy)_2Ru(dpp)Ru]^+$ was consistently identified. However, the DHC matrix did not generate such a species. The role of the deposition solvent (acetone or acetonitrile) had little effect on the spectra for any given matrix.

With the DHC matrix, more laser shots could be averaged before the ion signals deteriorated. Averaging was possible for up to 75 shots when the defocused laser beam was used, and the noise of the spectra was reduced. The laser energies required for ionization were slightly less (approximately 10%) for the focused- versus the defocused-beam ablation techniques. The co-crystallization of the matrix with the analyte influenced the ability to generate quality mass spectra, since the denser DHC crystals facilitated finding a “good irradiation spot”.

Table VI. 3: Summary of the ions observed in the analysis of the $\{[(bpy)_2Ru(dpp)]_2RuCl_2\}(PF_6)_4$ compound.

$\{[(bpy)_2Ru(dpp)]_2RuCl_2\}(PF_6)_4$ ("Tri-Ru") RESULTS

DIRECT ABLATION	Tri-Ru in 2,5 DHB matrix	Tri-Ru in 3,4 DHC matrix
100-104	--	--
107 (small)	--	--
234	235	235
~257 (small)		
~334	~334	~334 (sm)
~414	~414	~414
~492	~492	~492
~570		
~649	~649	~649
	~750	

PROBABLE IDENTIFICATIONS OF THE MAJOR ION PEAKS

MASS (amu)	STRUCTURE
100-104	Ruthenium isotopes
107	PF_4^+
157	bpy^+
234/235	dpp^+ / $(dpp + H)^+$
~257	$Ru(bpy)^+$
~334	$Ru(dpp)^+$
~414	$Ru(bpy)_2^+$
~491	$Ru(bpy)(dpp)^+$
~570	$Ru(dpp)_2^+$
~649	$Ru(bpy)_2(dpp)^+$
~750	$Ru(bpy)_2(dpp)Ru^+$

VI.10-- $\{[(bpy)_2Ru(dpp)]_2IrCl_2\}(PF_6)_5$ ("JSB") RESULTS

With the insight gained from the studies of the $[Ir(dpp)_2Cl_2](PF_6)$ and the $\{[(bpy)_2Ru(dpp)]_2RuCl_2\}(PF_6)_4$ complexes, observations and spectra from the heteronuclear trimetallic $\{[(bpy)_2Ru(dpp)]_2IrCl_2\}(PF_6)_5$ can be better understood. This target compound of our investigations will probe all aspects of our mass spectrometric analysis (i.e. bond strengths and fragility under laser ablation, ionization mechanisms, fragmentation reactions, sample preparation, etc.). Also, some instrumental modifications would be made, allowing an investigation of the time-scale of fragmentation.

VI.10.1-- Direct Ablation

The simplest sample preparation method, direct-deposition of the analyte into the sample cup, yielded significant fragmentation upon laser ablation. Operation over laser energies of approximately 20 μJ extensively dissociated the compound, made peak identification difficult, and lowered the S/N ratio due to multiple losses of C, H, and N from the ligand molecules. Threshold laser energies were similar to that of the $\{[(bpy)_2Ru(dpp)]_2RuCl_2\}(PF_6)_4$ and $[Ir(dpp)_2Cl_2](PF_6)$ compounds (~5 μJ).

As the results summary in Table VI.4 shows, the molecular ion could not be observed, and fragmentation of the analyte produced an abundant number of ions, especially in the low-mass region (see Figure VI.13). Most of the low-mass peaks result from the dissociation of various ratios of C, H, and N from the ligands. Similar to the direct laser ablation of the $\{[(bpy)_2Ru(dpp)]_2RuCl_2\}(PF_6)_4$ and $[Ir(dpp)_2Cl_2](PF_6)$ analytes, the PF_4^+ species was detected in high laser energy $\{[(bpy)_2Ru(dpp)]_2IrCl_2\}(PF_6)_5$ spectra. This may be attributed to a retention of the oxidation state of the cation (P(V)), with F^- displacements from the PF_6^- counterion. Also, a thorough investigation of the high-energy formation of bare Ru^+ ions (~100 amu) revealed a good comparison with the known isotopic ratios. The presence of the Ru^+ isotopes contrasts the lack of the bare Ir^+ species in $[Ir(dpp)_2Cl_2](PF_6)$ spectra, and might reveal decreased ionization efficiencies for iridium. Ion yields of each of the bare ligands

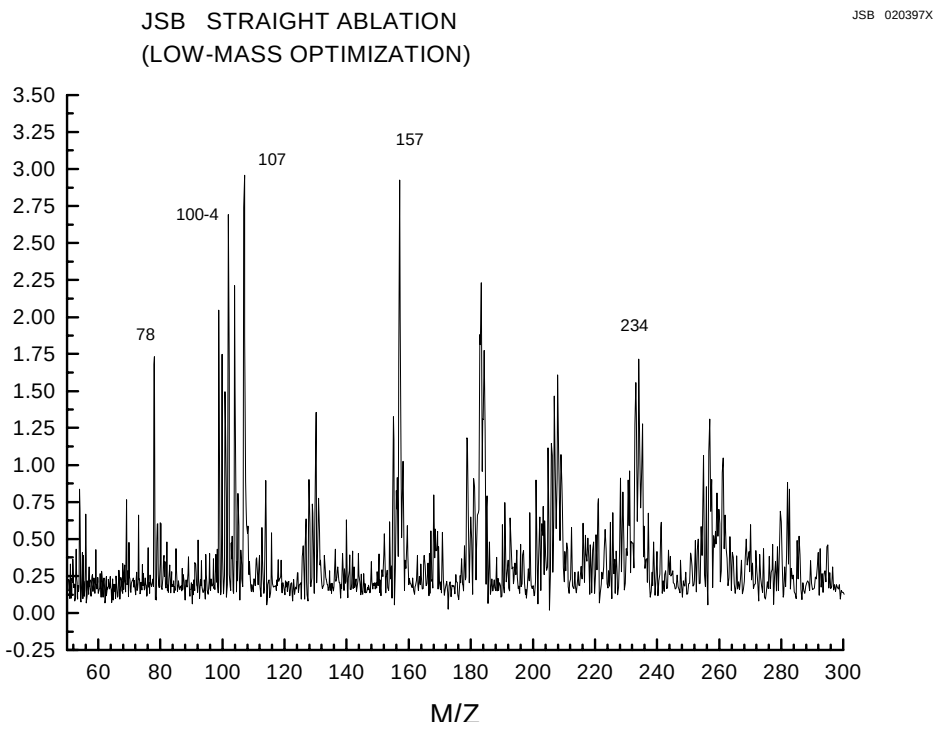

Figure VI. 13: {[(bpy)$_2$Ru(dpp)]$_2$IrCl$_2$(PF$_6$)$_5$} ("JSB"); Typical spectrum of a straight ablation sample (TOF-MS conditions optimized for the 50-300 amu region).

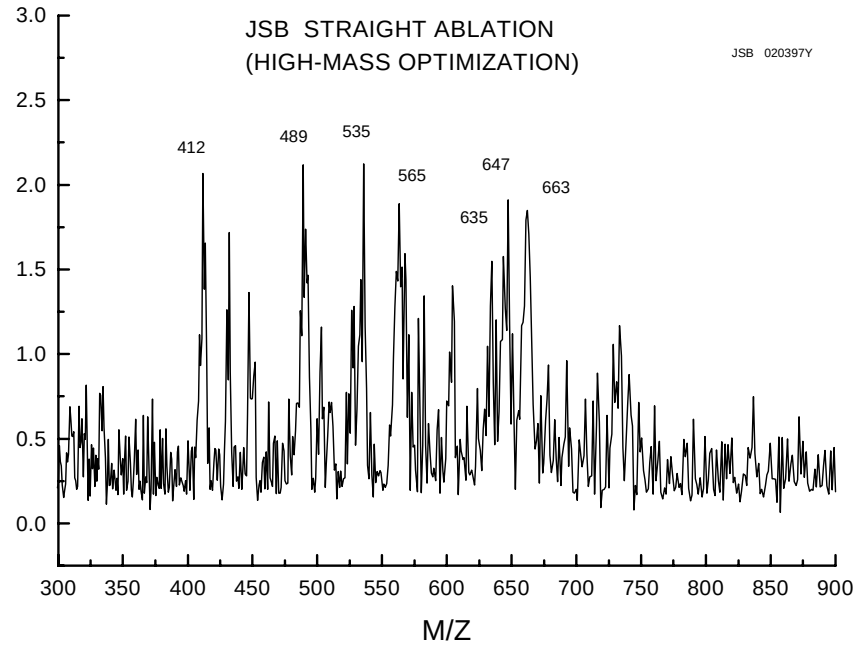

Figure VI. 14: {[(bpy)$_2$Ru(dpp)]$_2$IrCl$_2$(PF$_6$)$_5$} ("JSB"); Typical spectrum of a straight ablation sample (TOF-MS optimized for ~300-900 amu region).

from the $\{[(bpy)_2Ru(dpp)]_2IrCl_2\}(PF_6)_5$ complex, dpp^+ and bpy^+ (234 amu and 157 amu, respectively) were high, and indicate the ease of ligand cleavage from the molecule.

In the higher-mass region, as shown in Figure VI.14, some important fragments of the molecule retaining the Ru-ligand(s) bonds remained intact. Notable fragments are attributed to Ru with each ligand or a combination of ligands, as shown in Table VI.4. A possible Ir-containing species, $[Ir(dpp)_2]^+$ (~660 amu), seems the only Ir moiety in the spectra and was observed only in low yields. However, the low relative yield of this signal might indicate that rearrangements or ligand transfers truly account for this peak. Analysis of the $[Ir(dpp)_2Cl_2](PF_6)$ complex implies that the ~660 amu peak would be accompanied by peaks at ~698 and ~733 amu. However, these peaks were not observed in $\{[(bpy)_2Ru(dpp)]_2IrCl_2\}(PF_6)_5$ spectra. All of the observed fragments may be important for structural studies of the compound, but improvements to the spectra through MALDI were necessary.

VI.10.2-- MALDI results with the $\{[(bpy)_2Ru(dpp)]_2IrCl_2\}(PF_6)_5$ complex

VI.10.2.1-- Sample preparation

Even wider varieties of sample preparation techniques were attempted with the heteronuclear, trimetallic $\{[(bpy)_2Ru(dpp)]_2IrCl_2\}(PF_6)_5$ compound. The direct-deposit method for straight laser ablation and the traditional MALDI mixture procedure using either acetone or ethanol as the solvent were used. In addition, a fast evaporation, "on top" method was tried. In this rapid approach, a concentrated solution of the matrix (~3 μL total volume dissolved in acetone) was pipetted into the sample cup and allowed to evaporate. Depositing approximately an equal amount of a concentrated solution of the $\{[(bpy)_2Ru(dpp)]_2IrCl_2\}(PF_6)_5$ analyte "on top" of the matrix followed.

In general, as long as a good crystal was found, the spectrum of an "on top" sample revealed similar fragmentation patterns to a mixture sample in the same matrix. For mixture samples, a comparison of the different sample:matrix ratios for a given matrix revealed that the exact ratio (~1:50 to 1:1000) did not greatly impact the ions observed. As expected, though, the intensity the $\{[(bpy)_2Ru(dpp)]_2IrCl_2\}(PF_6)_5$ peaks compared to the matrix ions was slightly less in the lower-ratio samples, and the signal again

deteriorated more rapidly. Similar to the other organometallic analyte samples, the MALDI spectra of $\{[(bpy)_2Ru(dpp)]_2IrCl_2\}(PF_6)_5$ with the 2,5-dihydroxybenzoic acid matrix exhibited the most rapid reduction of analyte ions upon repeated ablation of the same crystal.

Solvent selection (acetone versus ethanol) impacted the $\{[(bpy)_2Ru(dpp)]_2IrCl_2\}(PF_6)_5$ spectra more than solvent selection (acetone versus acetonitrile) for the $\{[(bpy)_2Ru(dpp)]_2RuCl_2\}(PF_6)_4$ compound. Most importantly, the crystallization of the ethanol-deposited $\{[(bpy)_2Ru(dpp)]_2IrCl_2\}(PF_6)_5$ samples was in most cases inferior to acetone-deposited samples upon visual inspection. The thinner ethanol-prepared crystals made "hunting" for a good laser spot difficult and time consuming. In addition, the quality of the mass spectra was poorer and consisted mainly of matrix ions, as a comparing Figure VI.15 with Figure VI.16 reveals . With similar TOF-MS conditions (repeller delays), the higher-mass fragments (over 400 amu) are significantly less abundant in the ethanol-prepared sample. The low-mass matrix ions, especially the major matrix peaks at 137 amu and 177 amu, are over three times as intense as the analyte ions. The solvent played an important role in the ions generated, and this is largely attributed to co-crystallization problems of $\{[(bpy)_2Ru(dpp)]_2IrCl_2\}(PF_6)_5$ in the ethanol solvent.

VI.10.2.2-- Comparison of matrices

The general choice of matrix used, whether the polar, H^+ transferring acids, or the non-polar, radical-forming (i.e. ionization via electron abstraction) 9-nitroanthracene, was a crucial factor governing the fragmentation and quality of the mass spectra. The poor results with the 9-nitroanthracene matrix reveal the incompatibility of the non-polar matrix with the polar $\{[(bpy)_2Ru(dpp)]_2IrCl_2\}(PF_6)_5$ analyte. Excessive fragmentation and a noted lack of higher-mass ions are clear from an analysis of Table VI.4 and Figure VI.17 (optimized for the ~ 200 to 700 amu region). Most notably, few ions over ~500 amu were observed, even when the TOF-MS was optimized for higher-mass species. In fact, the extensive yield of smaller-mass ions in the 250 amu to 500 amu region was remarkably similar to the direct ablation sample.

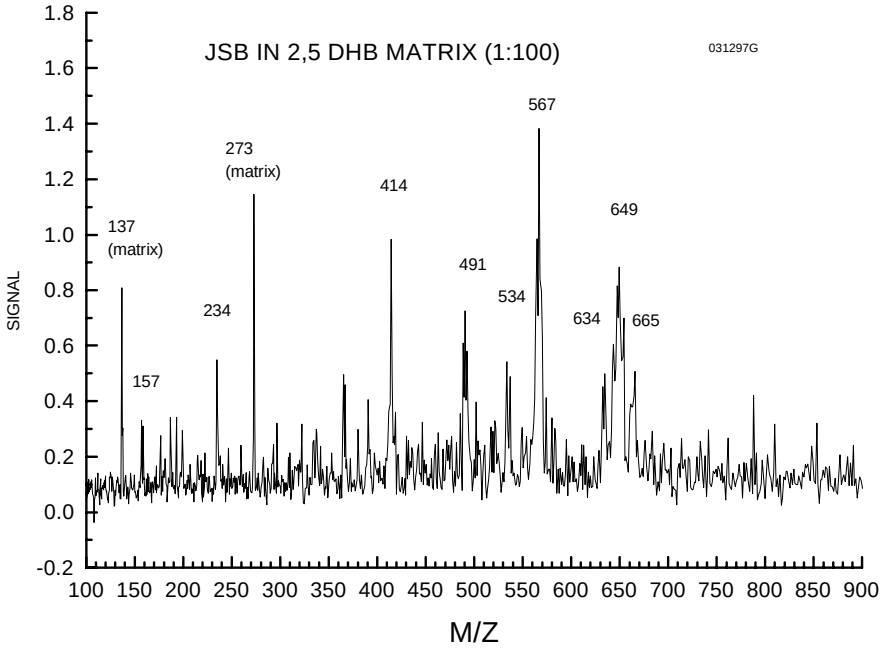

Figure VI. 15: {[(bpy)$_2$Ru(dpp)]$_2$IrCl$_2$(PF$_6$)$_5$} ("JSB"); MALDI spectrum of a sample prepared in DHB matrix.

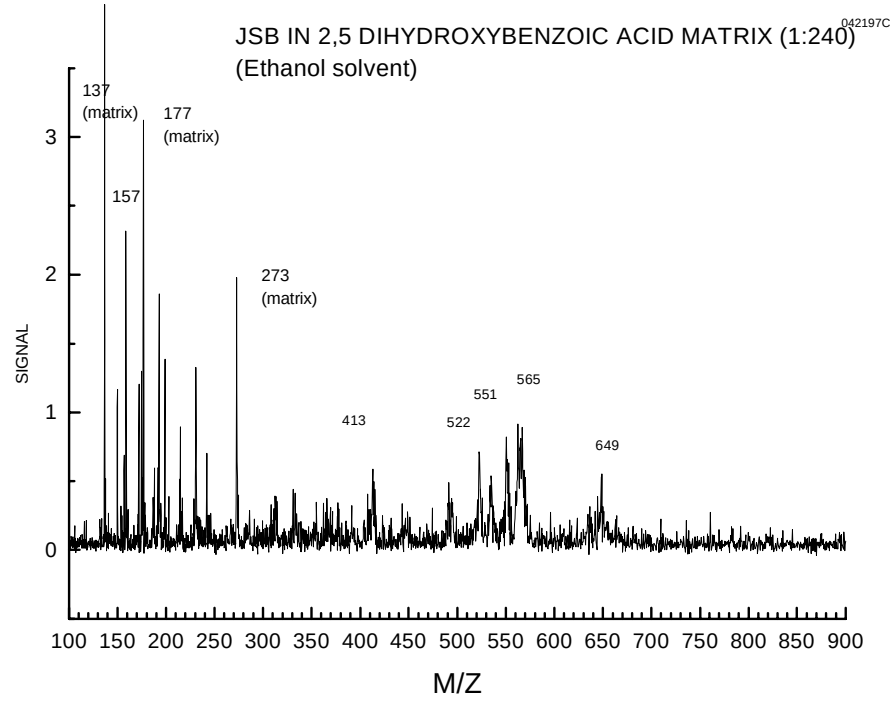

Figure VI. 16: {[(bpy)$_2$Ru(dpp)]$_2$IrCl$_2$(PF$_6$)$_5$} ("JSB"); MALDI spectrum of a sample prepared in DHB with ethanol solvent.

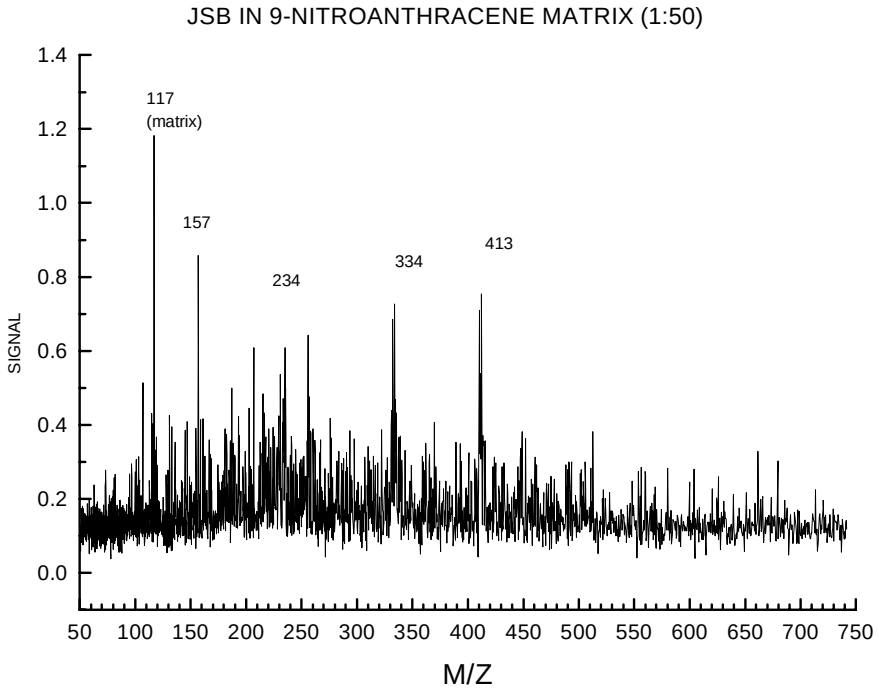

Figure VI. 17: {[(bpy)$_2$Ru(dpp)]$_2$IrCl$_2$(PF$_6$)$_5$} ("JSB"); MALDI spectrum of a sample prepared in 9-nitroanthracene matrix (TOF-MS optimized for ~200-700 amu region).

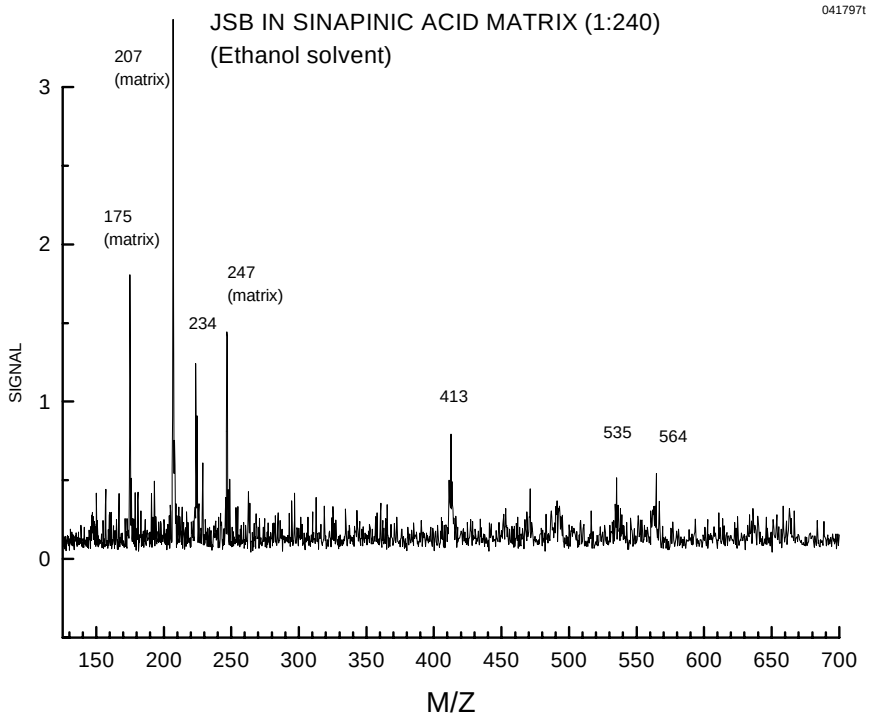

Figure VI. 18: {[(bpy)$_2$Ru(dpp)]$_2$IrCl$_2$(PF$_6$)$_5$} ("JSB"); MALDI spectrum of a sample prepared in sinapinic acid matrix with ethanol solvent (TOF-MS optimized for ~200-700 amu region).

Although it is an acidic matrix, unsuccessful results were also obtained with the sinapinic acid matrix. The visible quality of the crystals formed from this matrix in acetone was so poor that only an ethanol-prepared sample was used. Like the other ethanol-prepared samples and the 9-nitroanthracene-matrix sample, ion signals from the analyte could only be produced after extensive laser beam rastering across the sample surface to find a good crystal for ablation. Even when some signal was detected with the sinapinic acid-prepared sample, the yield of higher-mass (>500 amu) was low, and a typical spectrum (see Figure VI.18) shows the distinct absence of the $(bpy)_2Ru(dpp)^+$ (~650 amu) species.

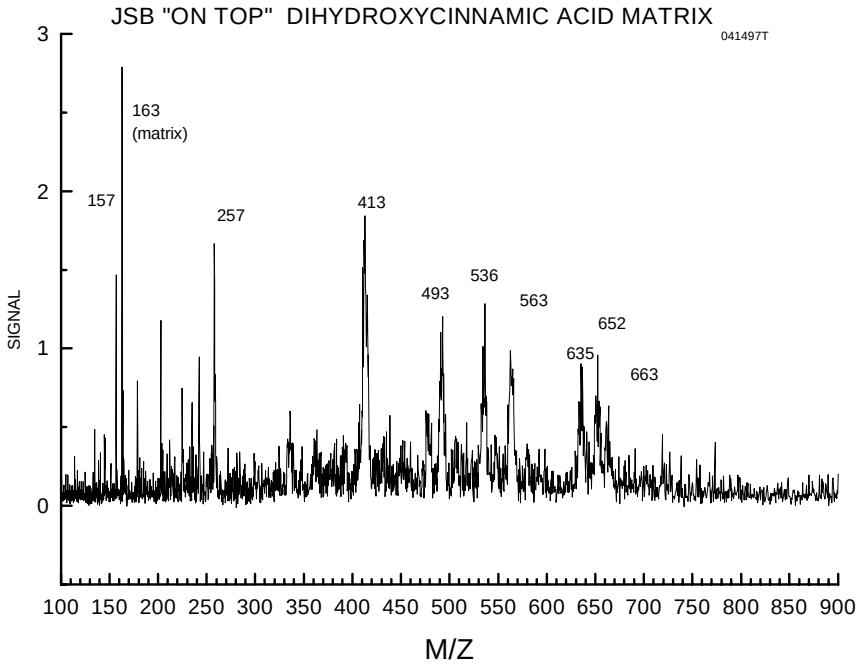

Figure VI. 19: $\{[(bpy)_2Ru(dpp)]_2IrCl_2(PF_6)_5\}$ ("JSB"); MALDI spectrum of a sample prepared with DHC matrix (TOF-MS optimized for ~300-900 region).

The ultimate goal of identifying the molecular ion was not attained with any of the MALDI matrices, but well-crystallizing, polar, proton-donating matrices improved the spectra considerably over the direct ablation samples. The best results were obtained with 2,5-dihydroxybenzoic acid and 3,4-dihydroxycinnamic acid matrices, which

promoted the yield of the larger-mass fragments (See Table VI.4). A comparison of the spectra of a direct ablation sample (Figures VI.13 and VI.14) with either the DHB (Figure VI.15) or DHC matrix (Figure VI.19) samples reveals the peak clarity of the high-mass ions and the higher S/N ratio for easier mass identification. Furthermore, the minimal laser beam repositioning to find a good sample crystal for laser revealed high-quality crystal formation.

VI.10.2.3-- Instrument modification

It is a distinct possibility that analyte fragmentation could occur after ejection from the sample surface in gas-phase collisions[90] before the ions are extracted from the TOF-MS ionization region and accelerated into the flight tube. Originally, the distance from the sample surface to the flight tube axis was ~4.0 cm (to center of flight tube of 2-cm diameter). Based on the optimum delay time preceding the repeller pulse, about 40 μs elapsed before ions were repelled into the flight tube, and the relatively long time spent in the ionization region might augment fragmentation. To address this possibility, extensions onto the sample probe of 1.65 cm and 2.50 cm were machined and samples were deposited (MALDI using 2,5-dihydroxybenzoic acid and, separately, 3,4-dihydroxycinnamic acid) on top of the extension. These two matrices were chosen because of the good results obtained from our previous studies, as highlighted above. The sample probe extensions succeeded in reducing the time preceding the repeller pulse to approximately 24 μs and 10 μs for the 1.65-cm and 2.50-cm extensions, respectively. These delay times were approximately three-fifths and one-quarter the time of the original repeller delays (~40 μs) when the probe extensions were not used.

The results of the samples placed on the probe extensions were nearly identical to the original configuration for both the DHB matrix and DHC matrix sample, with similar fragmentation patterns and relative ion yields. Thus, it is likely that fragmentation occurs almost instantaneously and near the sample surface (at least within the maximum bounds of 1.7-cm travel height, and within 10 μs). These findings are to be expected, since the microplasma jet, which forms upon laser irradiation, is largely confined to the sample surface and rapid cools above from the surface. However, firm conclusions should not be drawn, as others have found that with MALDI of protein samples, the use of a prompt

extraction reduced fragmentation over delayed extraction[89]. Also, the intact molecular ions may fragment in the drift tube[89,97] or in the reflectron.

VI.10.2.4-- Discussion

The target compound of our analysis, $\{[(bpy)_2Ru(dpp)]_2IrCl_2(PF_6)_5\}$ ("JSB"), was thoroughly analyzed under a variety of direct laser ablation and MALDI conditions. The molecular or pseudomolecular ions were not observed, revealing that fragmentation of this fragile complex preceded the ionization of the intact molecule. We successfully ionized and detected a complete ruthenium side unit and large fragments of the molecule, although the low abundance of iridium-containing fragments (i.e. the low-intensity peak ~660 amu) is curious. The results from the $[Ir(dpp)_2Cl_2](PF_6)$ complex reveal that iridium-containing fragments can be ionized and detected, so one possibility for the abundance of $Ru(ligand)^+$ ions in the $\{[(bpy)_2Ru(dpp)]_2IrCl_2\}(PF_6)_5$ spectra is the preferential ionization of ruthenium-containing species over iridium-containing species. Another possible reason is an ease of fragmentation of Ir-containing species. These findings depict the importance of the central metal atom in governing ionization and fragmentation processes[84,98]. The ions observed in the $\{[(bpy)_2Ru(dpp)]_2IrCl_2\}(PF_6)_5$ spectra all appear to be singly charged species and readily identifiable as fragment ions of the molecule. Again, analysis of the related compounds aided in this conclusion, especially the similar fragmentation patterns of the $\{[(bpy)_2Ru(dpp)]_2RuCl_2\}(PF_6)_4$ complex.

Using of the sample probe extensions also assessed the time scale of fragmentation. Although the time before ion extraction was reduced to as low as ~10 μs, fragmentation was still observed. Thus, it appears that the laser-induced microplasma disrupts the bonds within the compound nearly instantaneously. Collisions at or near the sample surface are likely.

[97] R. Brown, J. Lennon. *Anal. Chem.* **67** (1995) 1998.
[98] Z. Liang, A. Marshall, J. Marcalo, N. Marques, A. de Matos, I. Santos. *Organometallics.* **10** (1991) 2794.

Table VI. 4: Summary of the ions observed in the analysis of the $\{[(bpy)_2Ru(dpp)]_2IrCl_2\}(PF_6)_5$ ("JSB") complex.

$\{[(bpy)_2Ru(dpp)]_2IrCl_2\}(PF_6)_5$ ("JSB") RESULTS

MATRICES AND PREPARATION CONDITIONS

MASS (amu)	1	2	3	4	5	6	7	8	9
78	X								
100-4	X								
107	X								
157	X	X	X	X	X	(sm)	X	X	X
234	X	X		X			X	X	X
~257	X		(sm)	(sm)					
~334	X		X	(sm)	(sm)			(sm)	X
~414	X	X	X	X	X	X	X	X	X
~431	X		X						
~447	X		X						
~490	X	X	X	X	X	X	X	X	X
~523					X	X			
~535	X	X		X	X				X
~566	X	X		X	X	X	X	X	X
~605	X								
~635	X	X		X		(sm)	X	X	X
~647	X	X		X	(sm)	(sm)	X	X	X
~664	X	X		X		(sm)	X	X	X
~695	X								

NOTES REFERRING TO Table VI. 4:

1. Notations: X = reliable, intense peak which appears in most spectra
   (sm) = "small"; peak is not as intense as others and does not show significantly in all spectra.
2. The larger-mass peaks are actually composed of several distinct peaks separated by 1 amu; the values in the table depict the most intense of the cluster
3. Confirmed matrix ion peaks and fragment ions in the 100-400 amu region of the straight ablation sample are omitted from the table.

Table VI.4 (cont.)

MATRICES AND SAMPLE PREPARATION CONDITIONS

1. Direct Ablation (acetone, ethanol)
2. 2,5 Dihydroxybenzoic acid (acetone)
3. 9-Nitroanthracene (acetone)
4. 3,4 Dihydroxycinnamic acid (acetone)
5. 2,5 Dihydroxybenzoic acid (ethanol)
6. Sinapinic acid (ethanol)
7. 2,5 Dihydroxybenzoic acid (+1.65 cm probe extension)
8. 2,5 Dihydroxybenzoic acid (+2.5 cm probe extension)
9. 3,4 Dihydroxycinnamic acid (+2.5 cm probe extension)

PROBABLE IDENTIFICATIONS OF THE MAJOR ION PEAKS

MASS (amu)	STRUCTURE
78	Pyridine
100-104	Ruthenium isotopes
107	PF_4^+
157	bpy^+
234/235	dpp^+ / $(dpp + H)^+$
~257	$Ru(bpy)^+$
~334	$Ru(dpp)^+$
~414	$Ru(bpy)_2^+$
~491	$Ru(bpy)(dpp)^+$
~566	$Ru(dpp)_2^+$
~649	$Ru(bpy)_2(dpp)^+$
~664	$Ir(dpp)_2^+$

MALDI sample preparation techniques largely dictated the fragmentation patterns of the analyte. Both the choice of matrix and the solvent used (ethanol or acetone) impacted the results, as is typical of MALDI analyses[87,90,92,93,94]. In the extreme example, the non-polar matrix 9-nitroanthracene did not efficiently ionize the larger $\{[(bpy)_2Ru(dpp)]_2IrCl_2\}(PF_6)_5$ fragments. Without an available H^+ to assist in ionization of the moieties, electron abstraction was insufficient for ionization. Similarly, the direct laser ablation of the sample, with electron abstraction again the dominant mechanism of ionization, could not generate high intensities of the larger fragments. The polar, proton-donating acidic matrices in most cases ionized the larger fragments more effectively. Distinct mass resolution of the ligand protonation (dpp + H^+) suggests that the donation of H^+ from a carboxyl group of the matrix ionizes the larger, metal-containing fragments. Even with the acidic matrices, samples prepared in ethanol were inferior to acetone. The lack of ionization of larger fragments and difficulties in finding a "good spot" for laser ablation reveal the importance of the crystallization process of the matrix with the analyte. Unfortunately, aside from the polar versus non-polar matrix selection, MALDI results with the different matrices was largely "trial-and-error"[94]. In general, though, the MALDI results, especially with the 2,5-dihydroxybenzoic acid and 3,4-dihydroxycinnamic acid matrices, reduced the low-mass fragments of the molecule, improved the S/N ratio of the spectra, and intensified the larger-fragment ions.

Several complications arose in the analysis of the $\{[(bpy)_2Ru(dpp)]_2IrCl_2\}(PF_6)_5$ complex. As with the other complexes, the numerous isotopes of the metal atoms lead to complicated spectra. The natural abundances of the Ru^+ and Ir^+ isotopes are so similar that for repeated laser shots, different peaks of the distribution were more intense than others. These similarities in mass also lead to spectral overlap, making the identification of H^+ donation difficult. In addition, the exact location of fragmentation cannot be confirmed. Fragmentation likely occurs near the sample surface or in the ionization region, as metastable decay in the flight tubes or reflectron should be indicated by times-of-flight that do not correspond to prominent fragments of the molecule. Because of the poor resolution of our instrument in linear mode, this issue could not be addressed further. Another instrumental difficulty is the dependence of ion extraction on the

repeller delays that are used. Inaccuracies may arise when comparing the ion yields of spectra with far different repeller delays, and spectra optimized for a particular mass region often show diminished signals for ions away from the optimized region. To correct for this problem, the repeller delay was varied in order to observe the range of ions generated.

VI.11-- OVERALL CONCLUSIONS

Although the molecular ion could not be produced from the heteronuclear trimetallic $\{[(bpy)_2Ru(dpp)]_2IrCl_2\}(PF_6)_5$ complex, strides were made in the analysis of high molecular mass inorganic compounds. The improvements to the spectra from MALDI are quite significant, and show that the range of MALDI applications can extend into the inorganic regime. Greater S/N ratios, increased stability and ionization of larger portions of the molecule, and more controllable fragmentation were achieved for all three of the samples analyzed. A more detailed understanding of the MALDI process as applied to inorganic species was obtained, including some assessments of the ionization mechanisms, compatible matrices and solvents, and sample preparation conditions. Most notably, the choice of solvent and matrix proved vital to the quality of the spectra, and is attributed to compatibility of the matrix and polar organometallic analyte in the co-crystallization process. Also, the location and time scale of fragmentation were addressed by varying the distance (and thus the time) between the laser ablation pulse and ion extraction into the mass spectrometer.

Other successes with the MALDI investigations should be noted. A significant accomplishment was the molecular ion generation (including the counterion) for the monometallic $[Ir(dpp)_2Cl_2](PF_6)$ compound. This species was completely characterized through identification of individual fragments of the molecule, the pseudomolecular ion, and successive anion losses. Typically, only nanogram quantities of each analyte were necessary for analysis, and the LI-TOF-MS technique was fairly rapid. For any given matrix and sample preparation conditions, the mass spectra were highly reproducible. Major fragments of the molecule could be readily identified, especially with well-chosen MALDI matrices.

Complete structural confirmation of the $\{[(bpy)_2Ru(dpp)]_2IrCl_2\}(PF_6)_5$ or $\{[(bpy)_2Ru(dpp)]_2RuCl_2\}(PF_6)_4$ complexes could not be made because of the lack of molecular ion generation. Fragmentation appears easy in the larger trimetallic systems, independent of the homonuclear or the heteronuclear structure. However, significant fragments of the molecule were reliably identified as separate entities. Some speculations for the low abundance of iridium-containing species in $\{[(bpy)_2Ru(dpp)]_2IrCl_2\}(PF_6)_5$ spectra are excessive dissociation and decreased ionization. Multiply charged ions were not detected following straight laser ablation or MALDI of any of the compounds.

Overall, LI-TOF-MS is a valuable tool in the analysis of high molecular weight inorganic complexes. The "unlimited" mass range of TOF-MS mates well for the analysis of large gas-phase ions. Removal of the analyte from the sample surface and ionizing it in an intact form seem the limiting factors of the technique.

Future investigations will concentrate on generating the molecular ion from the organometallic complexes. MALDI should assist in this aspect, and more studies should take advantage of MALDI-TOF for the structural characterization of multimetallic inorganic species. In addition, varying the laser wavelength might reduce some resonance-ionization of the analyte to make laser ablation and MALDI even "softer" for these fragile molecules.